Acarologia
Open Science in Acarology

Gonads and gametogenesis in *Chaetodactylus osmiae* (Acariformes: Astigmata: Chaetodactylidae) a parasite of solitary bees

Elżbieta Rożej-Pabijan[a] , Wojciech Witaliński[b]

[a] Institute of Biology, Pedagogical University, Podchorążych 2, 30-084 Kraków, Poland.
[b] Department of Comparative Anatomy, Institute of Zoology and Biomedical Research, Jagiellonian University, Gronostajowa 9, 30-387 Kraków, Poland.

ABSTRACT

Chaetodactylus osmiae (Dufour, 1839) is a mite parasitizing the solitary bee – *Osmia rufa* L.– used as a commercial pollinator. In this study we present the anatomy of female and male reproductive systems of this species as well as its gonadal structure and gametogenesis at the ultrastructural level. The reproductive systems are similar to those of other Astigmata. The ovaries are paired and each contains germ-line cells – a giant nutritive ovarian cell connected via funnel-type intercellular bridges to oogonia and previtellogenic oocytes. Germinal cells are embedded in several large somatic stroma cells. Numerous protrusions of the nutritive ovarian cell penetrate into the stroma cell cytoplasm. Conspicuous ER cisterns run close and parallel to the surface of the germinal cells. Oocytes entering vitellogenesis disassociate with the nutritive cell and a vitelline envelope composed of heterogeneous material appears on their surface. When vitellogenesis is completed, the oocytes are full of lipid droplets and two types of yolk spheres; the vitelline envelope transforms into a thin and homogeneous chorion.

Paired testes are located on one side of the body, whereas the opposite side is filled by a male accessory gland. In testis, germinal cells are embedded in a few somatic stroma cells. The earliest spermatogonia form a compact germarium, whereas later stages are dispersed randomly within the testis. Spermatocytes are characterized by a superficial spongy layer, formation of mitochondrial derivatives, loss of the nuclear envelope and condensation of chromatin in threads. A single electron-dense lamella appears during the spermatid stage, separating chromatin threads from a large spongy body surrounded by arcuate, double-membrane bounded cisterns. In spermatids, the superficial spongy layer is absent. The testicular central cell in the germarium and structures related to meiotic division were not observed in the testes.

Spermatozoa are multiform cells (approx. 4×11µm) containing electron-dense lamella (ca. 45 nm thick) surrounded by mitochondrial derivatives which separate chromatin threads 45-50 nm thick from remnants of the spongy body *i.e.* arcuate cistern profiles. Spermatozoa deposited in female spermatheca are more electron dense; the electron-dense lamella is deeply folded several times, whereas chromatin threads are present in the center of the spermatozoon and are either flanked by lamella folds or located more peripherally under the plasmalemma. Remnants of the spongy body are not discernible.

Keywords ovarian nutritive cell, intercellular bridges, ovary, oogenesis, vitellogenesis, testis, spermatogenesis, spermatozoa, gonadal somatic cells, solitary bee parasite, Acariformes

Received 15 December 2017
Accepted 28 May 2017
Published 11 September 2018

Corresponding author
Elżbieta Rożej-Pabijan:
elarozej@vp.pl

Academic editor
Michel Bertrand

DOI
10.24349/acarologia/20184269

Copyright
Rożej-Pabijan E. and Witaliński W.

Distributed under
Creative Commons CC-BY 4.0

OPEN ACCESS

How to cite this article Rożej-Pabijan E. and Witaliński W. (2018), Gonads and gametogenesis in *Chaetodactylus osmiae* (Acariformes: Astigmata: Chaetodactylidae) a parasite of solitary bees. **Acarologia 58(4): 801-824; DOI 10.24349/acarologia/20184269**

Introduction

Managed pollinators such as solitary bees and bumblebees play an important role in fruit and vegetable production (Velthuis and Van Doorn 2006). Recently, solitary bees have been in focus, mainly those belonging to the *Osmia* genus. They are successfully used for pollinating early-spring fruit orchards. However, natural populations of *Osmia* are declining as a result of multiple factors (Krunić *et al.* 1995; Krunić *et al.* 2005). Astigmatic mites from the Chaetodactylidae family (suborder Hemisarcoptoidea) are serious pests of managed populations of *Osmia cornuta* and *O. rufa* in Europe (Bosch 1992; Krunić *et al*. 2005). In the Palearctic, the best known and most important is *Chaetodactylus osmiae* (Dufour, 1839) while *Ch. krombeini* plays a similar role in the Nearctic (OConnor and Klimov 2009; Klimov *et al.* 2016). Recent work indicates that these taxa may be further differentiated into two pairs of sibling species, *Ch. osmiae* and *Ch. claudus* in the Palearctic, and *Ch. krombeini* and *Ch. claviger* in the Nearctic, probably related to recent vicariance within the genus (OConnor and Klimov 2009).

Chaetodactylus osmiae has several life stages (egg, protonymph, deutonymph, tritonymph, adult male/female) (Michael 1903; Fain 1966; Van Asselt 2000), but most peculiar for the genus is the deutonymphal stage which can be observed in two morphotypes, an immobile form within the protonymphal exuvium and a mobile form, the so-called heteromorphic deutonymph (hypopus) (for further details see: Stanisavljević 1996; Krunić *et al.* 2005). The immobile deutonymph develops before autumn and allows the survival of mites through the colder part of the year, whereas the mobile deutonymph is a dispersal stage and uses phoresy to colonize new areas and hosts. The deutonymphal stages do not feed. Many experimental observations on *Ch. osmiae* biology were provided by Chmielewski (1993) and Stanisavljević (1996).

The relationships between *Ch. osmiae* and bees are complex. Although the active mite stages do not feed on bees, they can be detrimental by eating collected pollen and nectar, thereby decreasing food availability (kleptoparasitism). Moreover, if abundant, the mites can compete with bees for space inside the nest, leading to considerable reduction of the cocoon (Krunić *et al.* 2001; Krunić *et al.* 2005). The attachment of numerous phoretic deutonymphs to bees severely impedes flight and inhibits foraging (Krunić *et al.* 2005). For these reasons *Ch. osmiae* is considered a parasite of solitary bees.

A number of synapomorphic traits of the reproductive system and gametogenesis of Astigmata (Witaliński 2014) support their monophyly (OConnor 1984, 2009; Norton 1998; Schatz *et al.* 2011). The female reproductive system consists of oogenetic (primary) and inseminatory (secondary) parts. The oogenetic part comprises paired ovaries, paired oviducts and an unpaired oviduct (sometime called a "uterus") which empties into the preoviporal chamber. The chamber opens by a primary genital orifice (oviporus). The inseminatory part consists of an inseminatory opening, inseminatory canal, spermatheca and two sperm-conveying cords leading to ovaries. In the male, paired testes, paired deferent ducts joined together in an unpaired ejaculatory duct emptying at the tip of the aedeagus (penis), are present. In addition, one or two accessory glands opening at the beginning of the ejaculatory duct may occur. The variability of reproductive systems, gonad structure and gametogenesis in Astigmata was reviewed by Witaliński (2014), who provided some preliminary observations on *Ch. osmiae.*

Materials and methods

Females and males of *Chaetodactylus osmiae* (Dufour, 1839) collected from *Osmia rufa* nests were processed as follows. After sex identification under a Nikon SMZ1000 stereomicroscope (Nikon Instruments Europe, Amsterdam, Netherlands), the specimens were immersed one by one into a droplet of Karnovsky's fixative (Karnovsky 1965) (mixture containing 2% formaldehyde and 2.5% glutaraldehyde in 0.1 M cacodylate buffer, pH 7.2) on a parafilm-coated microscopic slide, the anterior part of the body was cut off with a fine razor blade

and the remaining rear part was transferred into fresh fixative for 24 h at 4°C. Fixed material was rinsed 4 x 15 min in 0.1 M cacodylate buffer containing 8% sucrose and postfixed with 1.4% osmium tetroxide in 8% sucrose overnight at 4°C. The specimens were then washed and dehydrated in a graded ethanol series followed by propylene oxide and embedded in Epon^{TM} 812 substitute (Sigma-Aldrich). Semithin and thin cross sections were sectioned on a Reichert-Jung ultramicrotome fitted with a diamond knife. Semithin sections on microscopic slides were stained with an Azur II and methylene blue (1:1) mixture, whereas thin sections were collected on formvar coated grids, contrasted with uranyl acetate and lead citrate according to standard protocols (Venable and Coggeshall 1965). Semithin sections were examined and documented under an Olympus BX51 microscope (Olympus Corporation, Tokyo, Japan), whereas thin sections were examined under a transmission electron microscope, JEOL JEM 100SX (JEOL Ltd., Tokyo, Japan), at 80 kV in the Department of Cell Biology and Imaging, Institute of Zoology and Biomedical Research, Jagiellonian University.

Results

1. The female reproductive system

The female reproductive system is comprised of oogenetic and inseminatory parts. The oogenetic part is composed of (1) paired ovaries located symmetrically in the most posterior part of the idiosoma (Fig.1B), (2) two oviducts possessing posteriorly-directed and anteriorly-directed sections, (3) the unpaired oviduct, and (4) a preoviporal chamber ending in (5) an oviporus. The inseminatory part consists of four elements. It begins with (1) an inseminatory opening located at the bottom of the tubular cuticular protrusion at the posterior end of the body (Fig. 1A-B), (2) a short funnel-shaped and cuticle-lined inseminatory canal (length ca. 43 µm, diam. from ca. 7 µm at inseminatory opening to ca. 36 µm at exit to spermatheca) leading to (3) a large spermatheca (120 x 200 µm, width x length) (Fig. 1B-F), and two very short (4) conveying cords connecting the basal part of the spermatheca with adhering ovaries.

2. The ovary

Each ovary (Fig. 1C-D) is composed of three cellular elements: one nutritive ovarian cell, previtellogenic oocytes, and several somatic stroma cells. The nutritive cell and oocytes are germ-line cells, whereas the stroma cells are somatic and fill narrow spaces between germ-line cells (Fig. 1C-D).

3. Nutritive cell and previtellogenic oocytes

The ovarian nutritive cell (Fig. 1C) is subspherical and very large (70 – 90 µm in diam.), and adheres to the postero-dorsal margin of the ovary. It is characterized by a giant multilobular nucleus with many distinct nucleoli (Fig. 2). The nuclear envelope contains many pore areas with adhering nuage material. The cytoplasm is full of ribosomes/ribosome subunits, crista-type mitochondria forming large and compact assemblages, multiform lysosomes and occasional Golgi bodies (Fig. 2). Most conspicuous for the nutritive cell is the formation of numerous protrusions penetrating deeply into the surrounding stroma cells (Fig. 3).

Previtellogenic oocytes are situated in the ventral part of the ovary below the nutritive cell (Fig. 1C), as well as in front of the nutritive cell (Figs 1D, 3A-B). They are irregular in shape and each oocyte is connected to the nutritive cell via a funnel-shaped intercellular bridge (Fig. 3A). The nucleus of small previtellogenic oocytes is irregular in shape due to the presence of many concavities on the envelope, containing nuclear pores. In advanced previtellogenic oocytes (Fig. 4), the nucleus is more spherical, with a number of shallow, pore-containing depressions of the envelope to which nuage material adheres (Fig. 4A-B). Nuage material in the nutritive cell and small previtellogenic oocytes is similarly fibrillar, but is more compact in advanced,

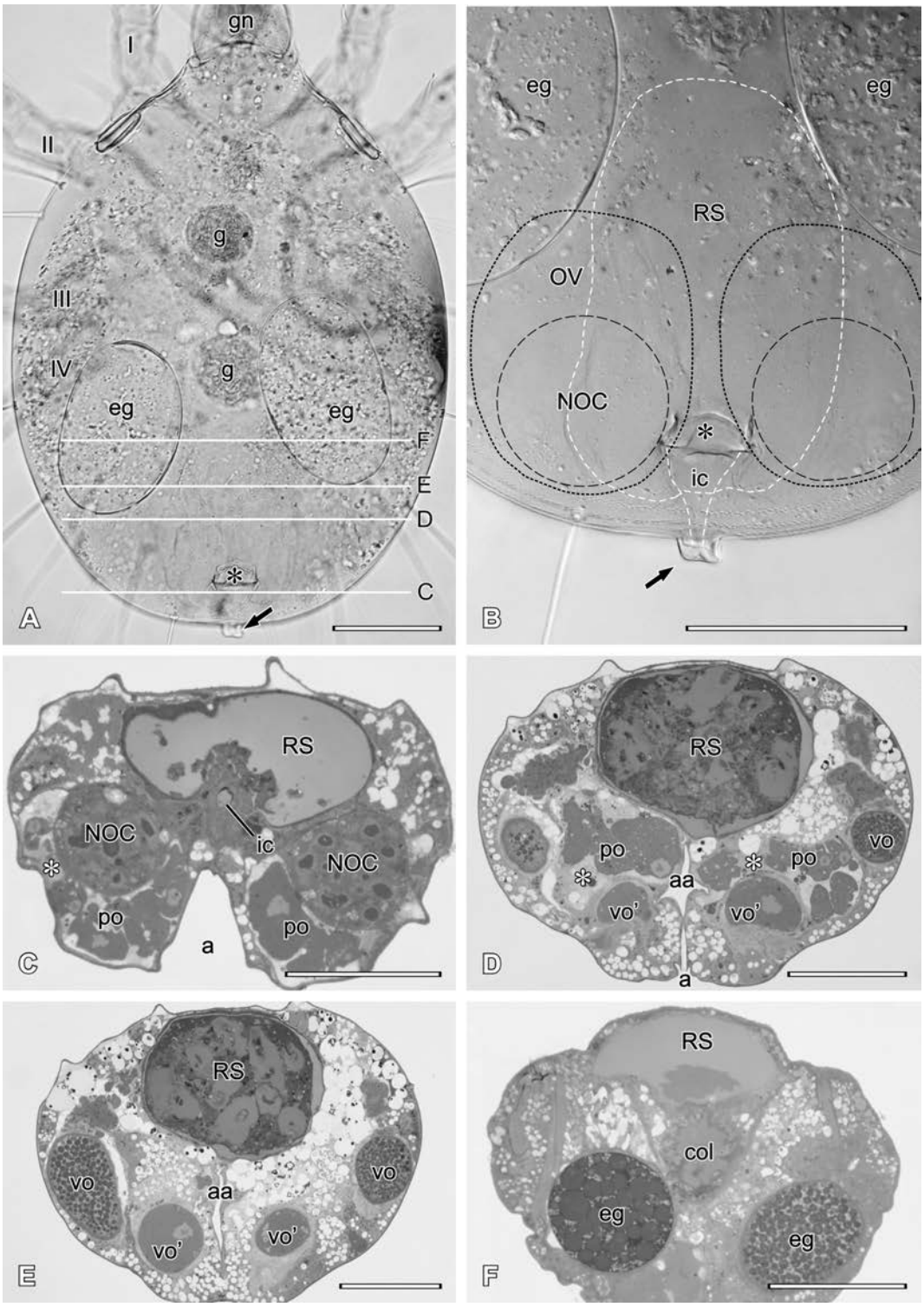


Figure 1 Light microscopic images of a *Chaetodactylus osmiae* female. Female in dorsal view (A) and the rear part of the idiosoma (B) with marked position of ovaries (OV), nutritive ovarian cells (NOC), spermatheca (*receptaculum seminis*) (RS) and inseminatory canal (ic). C-F – Semithin cross sections of idiosoma marked approx. at levels on (A). Note the spherical shape of nutritive cells (NOC) and irregular, wrinkled outline of previtellogenic oocytes (po) (C, D). Early vitellogenic oocytes (vo') located in the backward running oviduct are spherical (D, E). More developed vitellogenic oocytes (vo) and eggs (eg) in the forward running oviducts show increasing yolk filling (D-F). In the central part of the spermatheca, sperm-containing material delivered by a male is present (D, E), whereas the posterior-most and the anterior part of the spermatheca are free of such material (C, F). Sperm-containing material also shows large, oval structures of medium density (D, E).. Scale bars: 0.1 mm.
Other abbreviations: I-IV – legs I – IV; black arrow – inseminatory opening; black asterisk – basal part of spermatheca; white asterisk – spaces in the ovary filled with stroma cells; a – anal slit; aa – anal atrium; col – postcolon; eg – oviductal egg surrounded by chorion; g – food enveloped by peritrophic membrane in alimentary tract; gn – gnathosoma; ic – inseminatory canal; NOC – nutritive ovarian cell; po – previtellogenic oocytes; RS – spermatheca (receptaculum seminis) filled with male-derived material containing spermatozoa; vo' – early vitellogenic oocyte in backward running oviduct; vo – advanced vitellogenic oocyte in forward running oviduct.

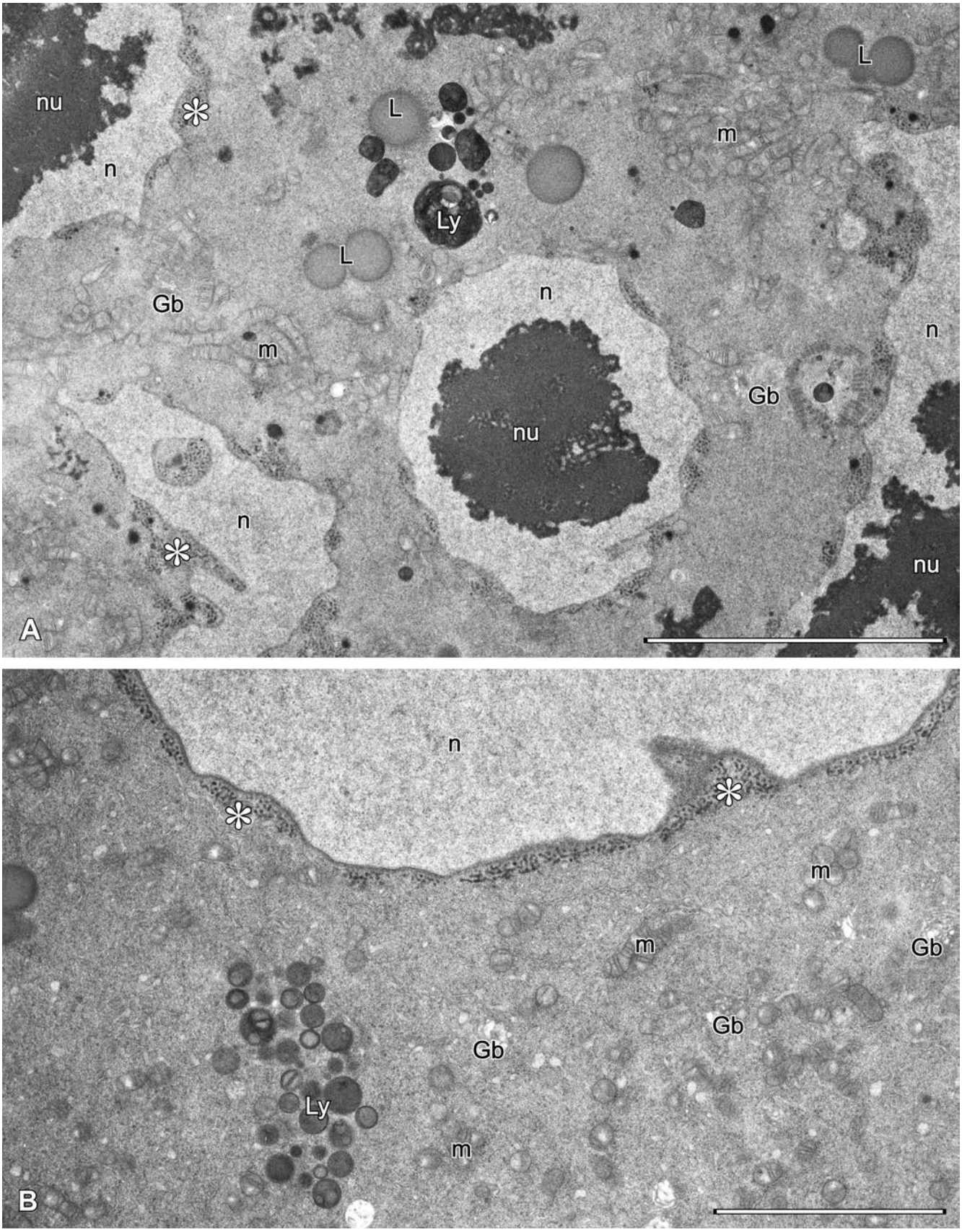


Figure 2 *Chaetodactylus osmiae* female, two aspects (A,B) of nutritive ovarian cell. TEM. Sections through multilobular nucleus (n) containing large nucleoli (nu). Cytoplasm filled with ribosomes also contains lipid droplets (L), many lysosomes (Ly), groups of mitochondria (m) and small vesicular Golgi bodies (Gb). Granular nuage material (asterisk) is usually present in concavities of the nuclear envelope. Scale bars: A – 10 μm, B – 5 μm.

larger previtellogenic oocytes (Figs 2, 3, 4A-B). In small previtellogenic oocytes, crista-type mitochondria tightly surround the nucleus, remaining in larger oocytes close to the nucleus (Fig. 3). Small Golgi bodies occur sporadically (Fig. 4B). Intercellular bridges are funnel-shaped and filled with electron-dense granules and microtubules in fan-like arrangements (Fig. 4D).

Stroma cells (Figs 3, 4A, C-D) fill all spaces between germinal cells; they are few in number and difficult to tally. Their electron-lucent cytoplasm contains ribosomes, ER profiles, mitochondria and groups of lysosomes. Stroma cells have characteristic subplasmalemmal ER cisterns (Figs 3A-B, 4A, C-D) running along the stroma cell/nutritive cell borders. Such cisterns are also present along larger protrusions of the nutritive cell, as well as along the surface of previtellogenic oocytes.

4. Vitellogenic oocytes and vitellogenesis

Oocytes entering vitellogenesis lose connection with the nutritive cell via intercellular bridges and are sequestered into the oviduct which starts ventrally at the anterior pole of each ovary. At first, the oviducts run posteriorly just below the ovaries then turn laterally and run anteriorly to eventually fuse into an unpaired oviduct. Thus, paired oviducts have backward-running and forward-running parts.

The oocytes in the oviduct become more spherical as they grow (Fig. 1D-E). Spherical nuclei are "empty" and have a centrally located nucleolus. In oocytes entering the second, forward-running part of the oviduct (Figs 1D-F, 5A-B), two types of inclusions can be discerned in the cytoplasm: lipid droplets usually associated with glycogen, and protein yolk spheres in different stages of condensation (Fig. 5A). At the beginning of yolk formation, large protein yolk spheres filled with moderately dense flocculent material are present (Fig. 5A). Later, their centers grow more dense to fill the yolk sphere completely. This yolk material is further concentrated, showing less condensed areas on a dense background. In some yolk spheres electron-light profiles with sharp edges can be seen; these are possibly remnants of crystalline inclusions removed during sample fixation for TEM (Fig. 5B).

5. Vitelline envelope and chorion

The vitelline envelope is formed on the surface of early vitellogenic oocytes. It is composed of material delivered from the cytoplasm via vesicles (Fig. 5A inset) and is layered rather than homogeneous, visible as alternating light and dark striae (Fig. 5A). As vitellogenesis proceeds, the vitelline envelope reorganizes and forms a much thinner and homogeneous layer, the chorion (Fig. 5B).

6. The male reproductive system

The male reproductive system in *Ch. osmiae* contains two testes, paired deferent ducts, an unpaired ejaculatory duct which opens at the tip of the aedeagus, as well as an unpaired accessory gland. Testes are located asymmetrically on the right side in the posterior part of the idiosoma: the right testis occupies a lateral position, whereas the left one is shifted dorsally (Fig. 7A). Depending on the specimen, the left testis may be longer and runs under the dorsal cuticle up to the level of the fourth coxae, or, alternatively, both testes can terminate earlier, close to the level of the aedeagus (compare Figs 6 and 7B).

The arrangement of deferent ducts is complicated. The left duct starts at the posterior end of the left testis then runs forward under the accessory gland to eventually pass to the right side in front of the anal atrium. The right duct appears ventrally in the central part of the right testis and runs antero-ventrally to fuse with the left deferent duct into the ejaculatory duct.

The ejaculatory duct (Figs 6B, 7B) is a tube (lumen diameter narrowing approx. from 6 µm to 2 µm) with cuticle lining, entering the aedeagus and opening at its tip (Fig. 6B).

A pyriform male accessory gland (diam. ca. 90-100 µm) (Fig. 7A) is located on the left side of the idiosoma and extends from the posterior end of the idiosoma up to the level of the coxae

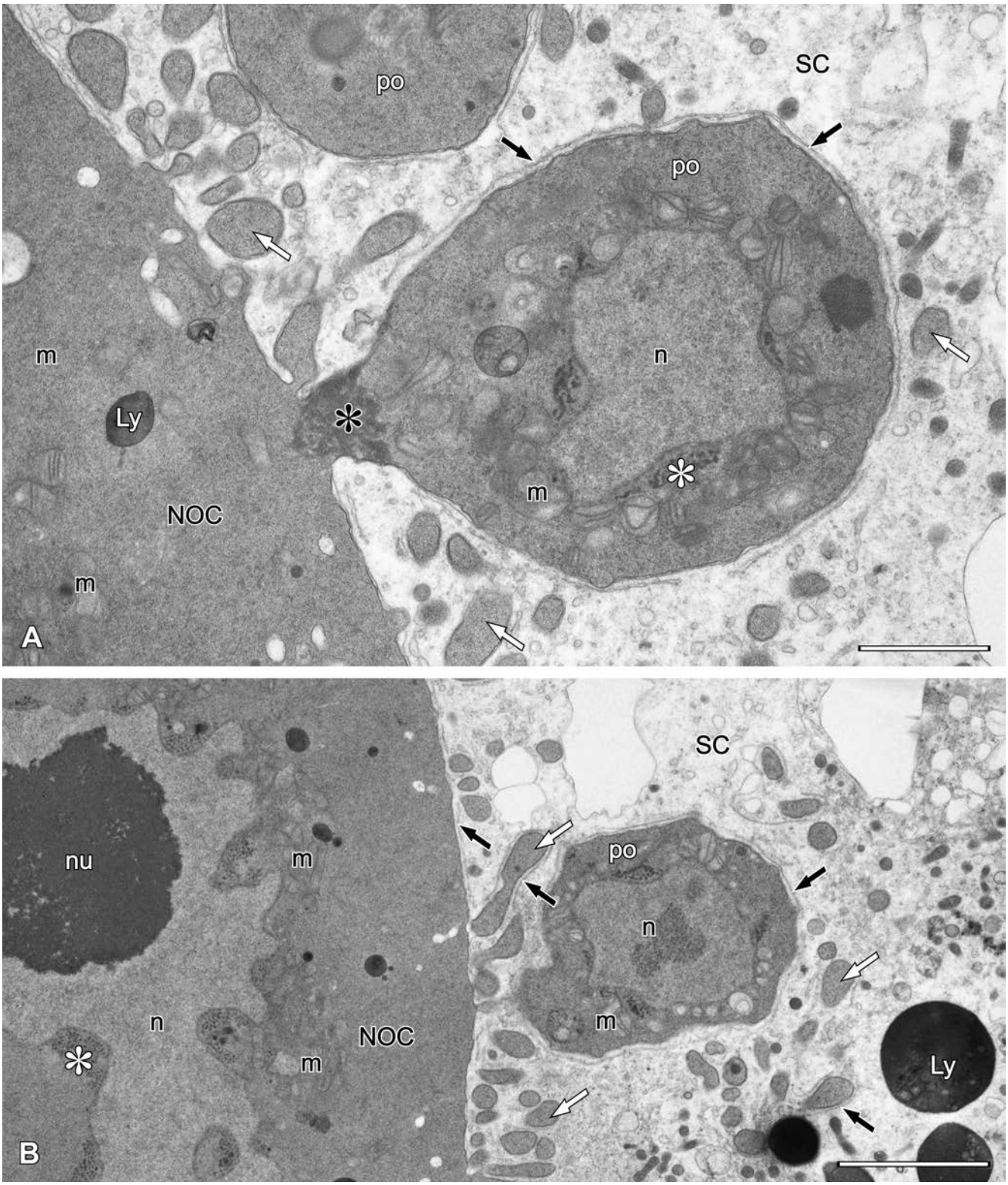


Figure 3 *Chaetodactylus osmiae* female, two aspects (A, B) of the peripheral part of the nutritive ovarian cell. TEM. (A) Nutritive cell (NOC) shows mitochondria (m) and lysosome (Ly), and is connected via an intercellular bridge (black asterisk) with an early previtellogenic oocyte (po). The other previtellogenic oocyte is partly visible above. The oocyte nucleus (n) is irregular in outline and envelope concavities contain electron dense nuage material (white asterisk). Mitochondria (m) in the oocyte closely surround the nuclear envelope. Somatic stroma cells (SC) show few ribosomes and are penetrated by many protrusions of a nutritive cell (white arrows). Note ER cisterns (black arrows) running in stroma cell parallel to its contacts with germ-line cells (i.e. nutritive cell and oocytes). (B) Another aspect of the nutritive cell periphery similar to (A). Note a lobe of the nucleus (n) with a nucleolus (nu) in the nutritive cell; concavities of the nuclear envelope are filled with nuage material (white asterisk) whereas mitochondria (m) are clustered close to the nucleus in both the nutritive cell and oocyte (po). Nutritive cell protrusions and ER cisternae in stroma cells are indicated by white and black arrows, respectively.
Other abbreviations: Ly – lysosome in stroma cell. Scale bars: A – 2 µm, B – 5 µm.

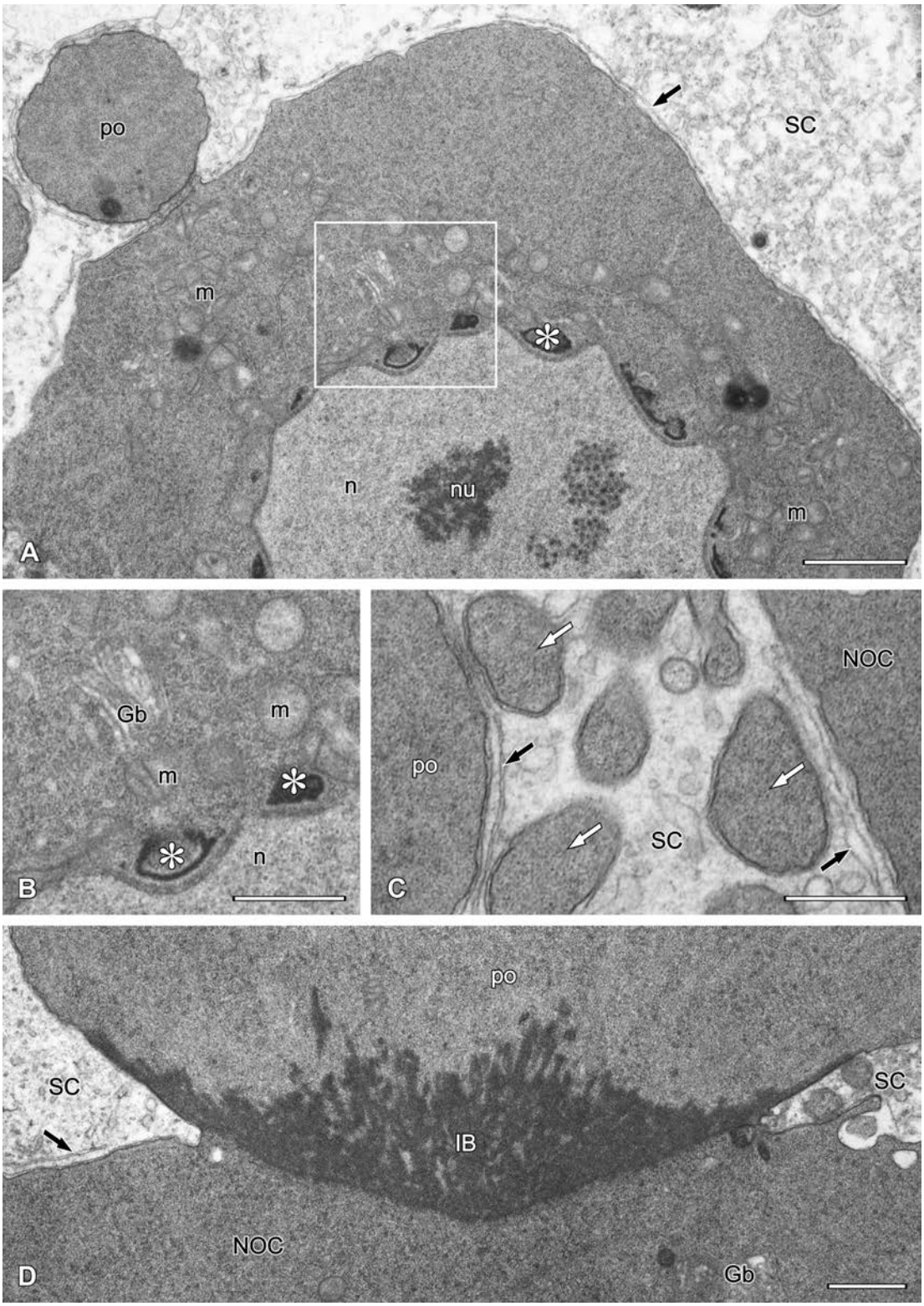


Figure 4 *Chaetodactylus osmiae* female. TEM. (A) Advanced previtellogenic oocyte showing nucleus (n) with nucleolus (nu). The nuclear envelope has concavities in sites rich in pores, with adhering nuage material (asterisk). Mitochondria (m) are grouped around the nucleus. Another oocyte sectioned tangentially (po) is also present. In the stroma cell (SC), an arrow marks a conspicuous ER cisterna. (B) Enlarged fragment of the oocyte marked in (A): note nucleus (n), a Golgi body (Gb), nuage (asterisks) and mitochondria (m). Note the different appearance of nuage material which is not granular as in the nutritive cell and early oocytes (compare with 2B and 3A-B).. (C) A gap between a nutritive cell (NOC) and previtellogenic oocyte (po) filled with a stroma cell (SC) in which several nutritive cell protrusions (white arrows) are embedded. ER cisterns in the stroma cell are also present (black arrows). (D) Intercellular bridge (IB) connecting a nutritive cell (NOC) and previtellogenic oocyte (po), filled with electron-dense granular material in fan-like arrangement. Golgi body (Gb) in nutritive cell and ER cistern (arrow) in stroma cell (SC) are marked. Scale bars: A – 2 µm, B-D – 1 µm.

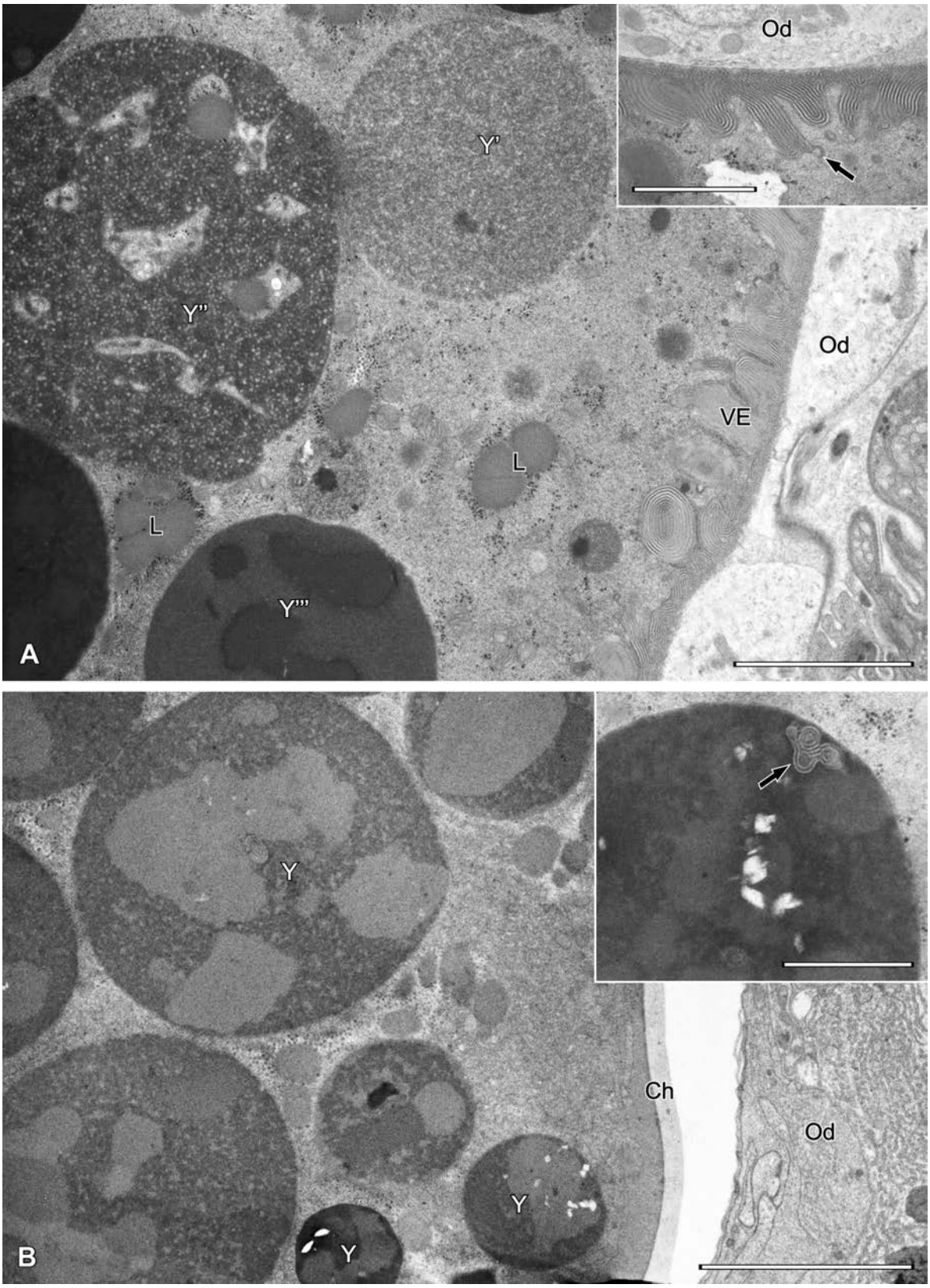


Figure 5 *Chaetodactylus osmiae* female. TEM. (A) Vitellogenic oocyte in upper (forward-running) part of oviduct (Od), containing yolk spheres in subsequent stages of development (Y', Y'' and Y''') and lipid droplets (L) surrounded by glycogen. Lamellar vitelline envelope (VE) covers the surface of the oocyte. Inset: Higher magnification of vitelline envelope adhering to oviduct (Od). Vesicle delivering vitelline envelope material from Golgi body is indicated by an arrow. (B) More advanced vitellogenic oocyte covered with thin and homogeneous chorion (Ch) in the upper oviduct (Od). Yolk (Y) spheres of two types, larger and less dense and smaller and more dense, containing cristalline electron-lucid inclusions. Inset: Yolk sphere with electron-lucid inclusions and meandering structure (arrow). Scale bars: A,B – 5 µm, A inset, B inset – 2 µm.

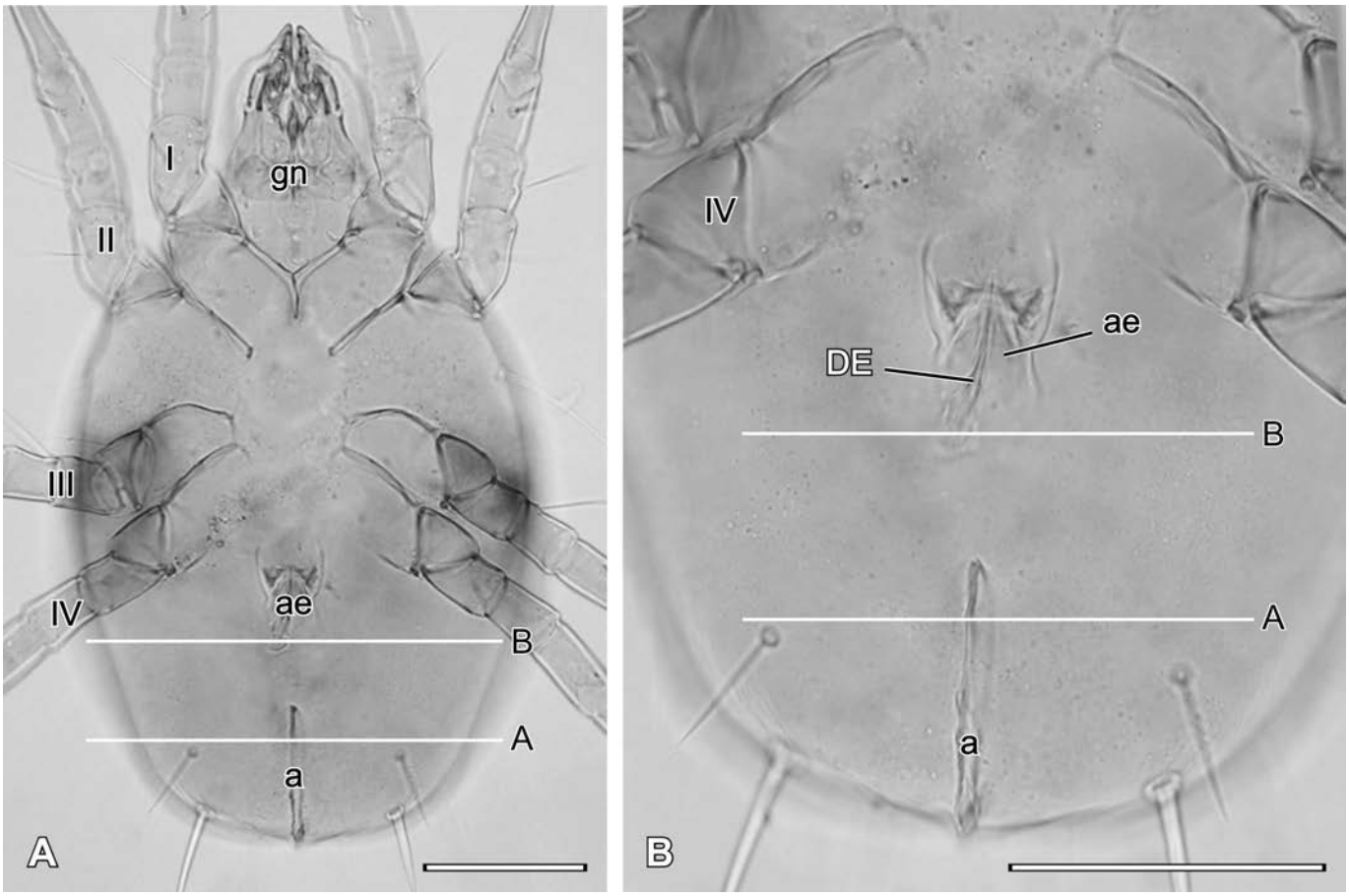


Figure 6 Light microscopic images of *Chaetodactylus osmiae* male. Male in ventral view (A) and the rear part of idiosoma (B). Scale bars: 0.1 mm. Abbreviations: I-IV – legs I-IV; lines A and B – levels of cross-sections in Figure 7; a – anal slit; ae – aedeagus; DE – ejaculatory duct; gn – gnathosoma.

of the fourth leg. The wall of the gland is variable in thickness and forms several concavities mainly in its rear part and along its dorsal surface. The lumen is filled with a homogeneous lucent material (Fig. 7A). The gland empties ventrally into the left deferent duct approximately at the level of the anterior margin of the anal atrium.

7. The testis

Testes are irregular in shape and contain male germ cells embedded in testicular stroma cells. In each testis early spermatogonia form a germarium (Fig. 7A-B) in which cells adhere tightly to each other (Fig. 8A-B). Cells that lose contact with the germarium proceed with spermatogenesis (Fig. 8B). Such cells disperse singly, thus the sequential distribution of stages of spermatogenesis is not maintained.

8. Spermatogenesis and sperm structure

The earliest spermatogonia that form the germarium (Fig. 8) are small polygonal cells (ca. 4.5 x 6.5 µm) tightly adhering to each other, with a spherical, relatively large nucleus containing a central nucleolus. The cytoplasm contains free ribosomes, crista-type mitochondria and occasionally visible Golgi bodies. Nuage material adhering to porous areas of the nuclear envelope also occurs.

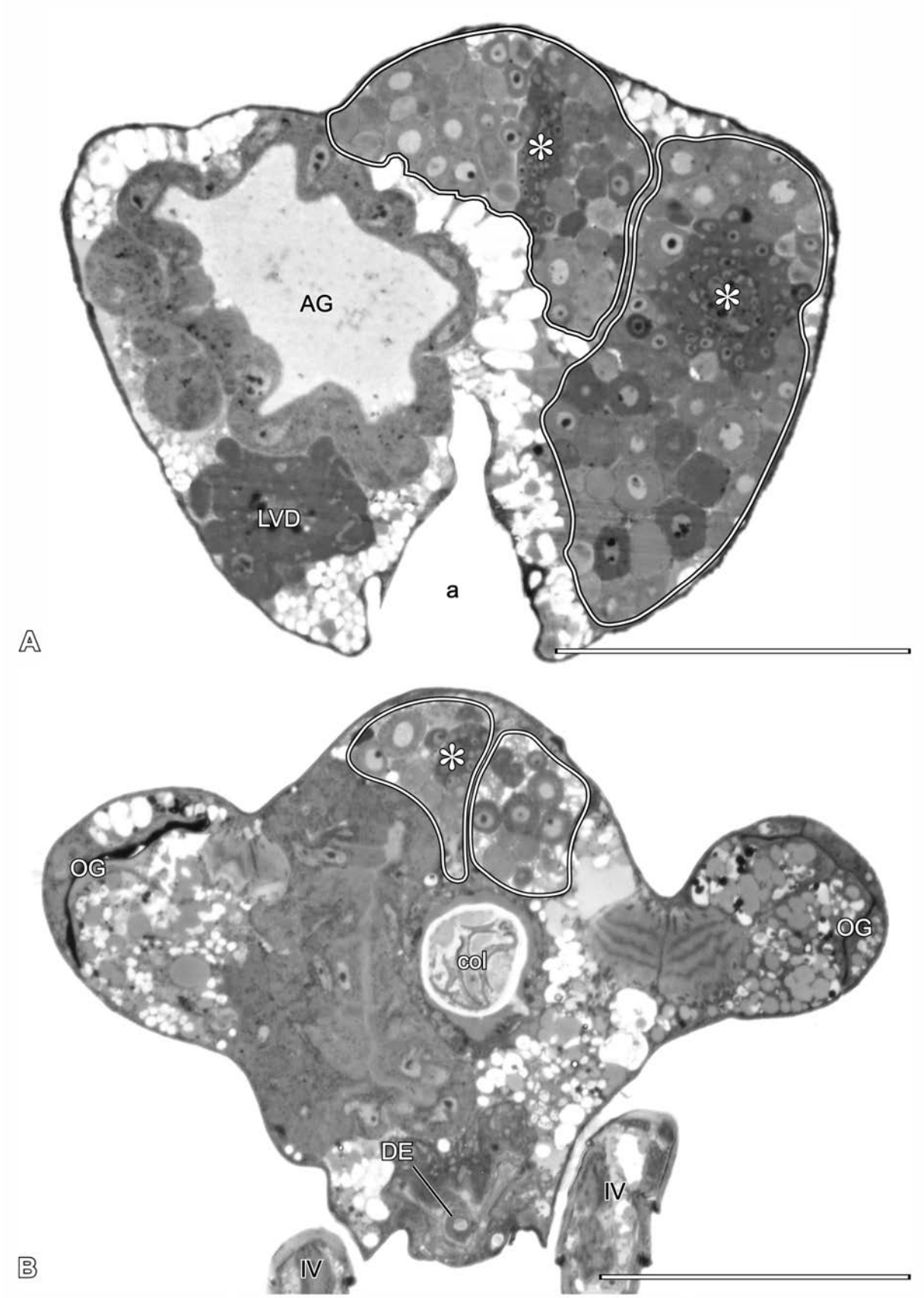


Figure 7 Light micrographs of cross sections through idiosoma of *Chaetodactylus osmiae* male at levels as indicated in Figure 6. Outlines of testes are marked. Scale bars: 0.1 mm.
Abbreviations: IV – leg IV; asterisk – germarium; a – anal slit; AG – male accessory gland; col – postcolon; DE – ejaculatory duct; OG – opisthonotal gland; LVD – left deferent duct.

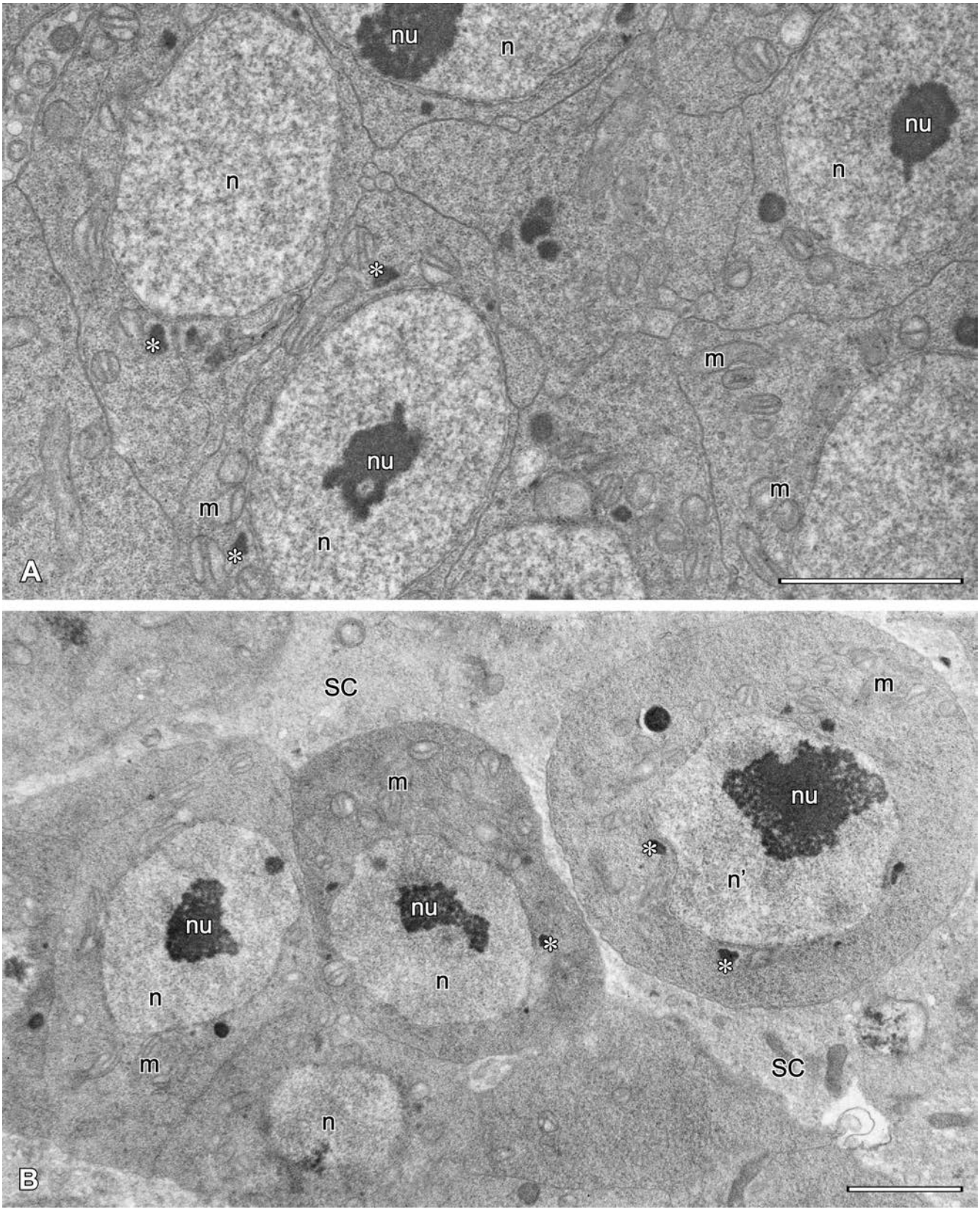


Figure 8 *Chaetodactylus osmiae* male, two aspects (A,B) of germarium. TEM. (A) Early spermatogonia assembled in germarium adhere tightly to each other. They possess a large nucleus (n) with prominent, usually central nucleolus (nu) and mitochondria (m) dispersed in the cytoplasm. Nuage material (asterisks) is present in several sites around the nuclei. (B) Early spermatogonia in germarium show features as in (A), whereas developing spermatogonium separated from germarium (right upper corner) is larger, roundish and has a larger nucleus (n') with peripheral nucleolus (nu). Spaces between developing spermatogonium and germarium are filled with a somatic stroma cell (SC). Scale bars: A – 2 μm, B – 5 μm.

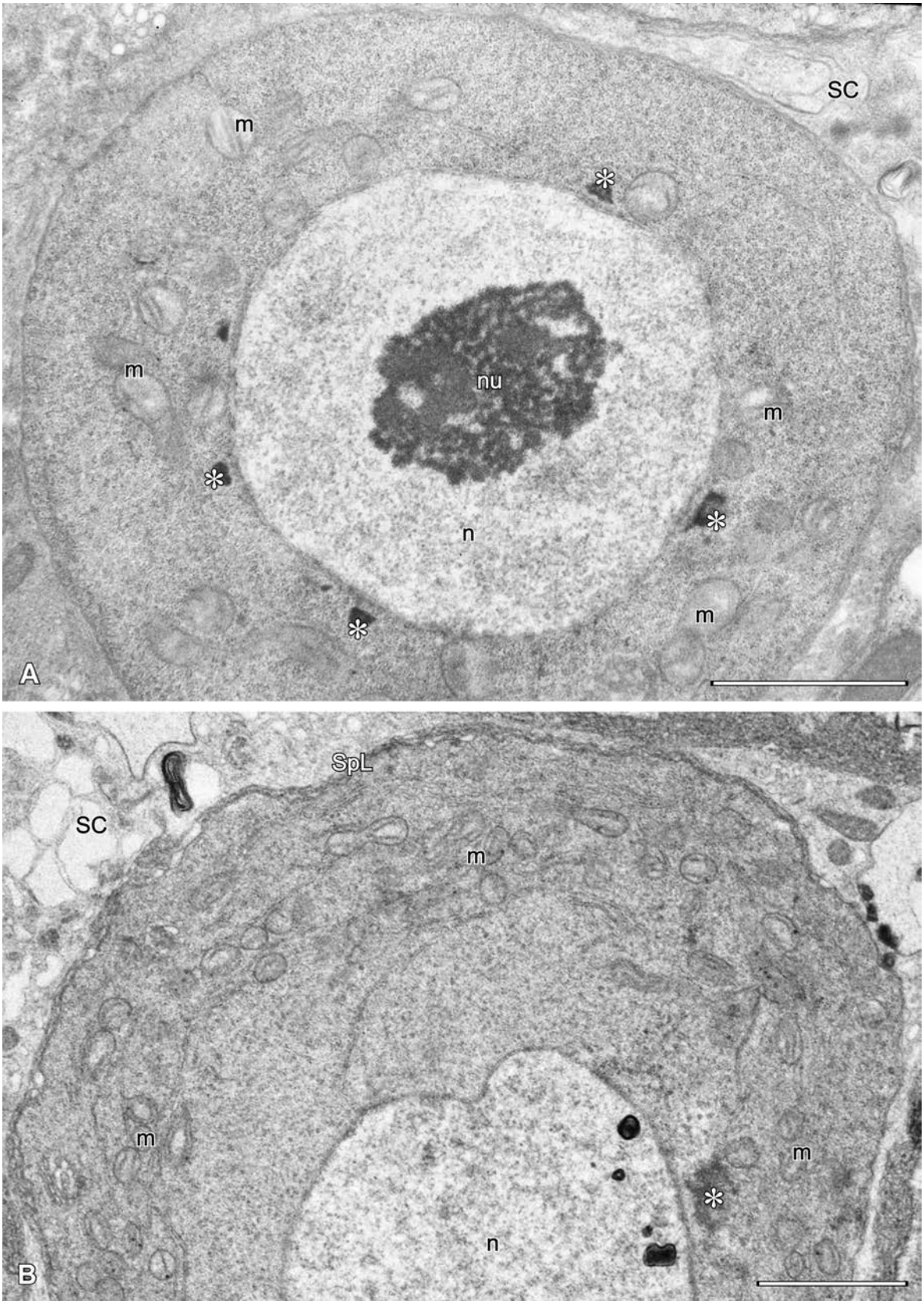


Figure 9 *Chaetodactylus osmiae* male. TEM. (A) Closer view of developing spermatogonium surrounded by a stroma cell (SC). Nucleus (n) is roundish and contains a prominent nucleolus (nu). There are a number of ribosomes in the cytoplasm, as well as dispersed mitochondria (m). Nuage material (asterisks) adheres to nuclear envelope in sites rich in pores. Note that the surface of the cell is smooth and not covered with a spongy layer. (B) Early spermatocyte showing spongy layer (SpL) at cell surface which is wrinkled and adheres to stroma cell (SC). Nuage material (asterisk) adheres to large nucleus (n). Numerous mitochondria (m) are located rather peripherally in the cell. Scale bars: 2 µm.

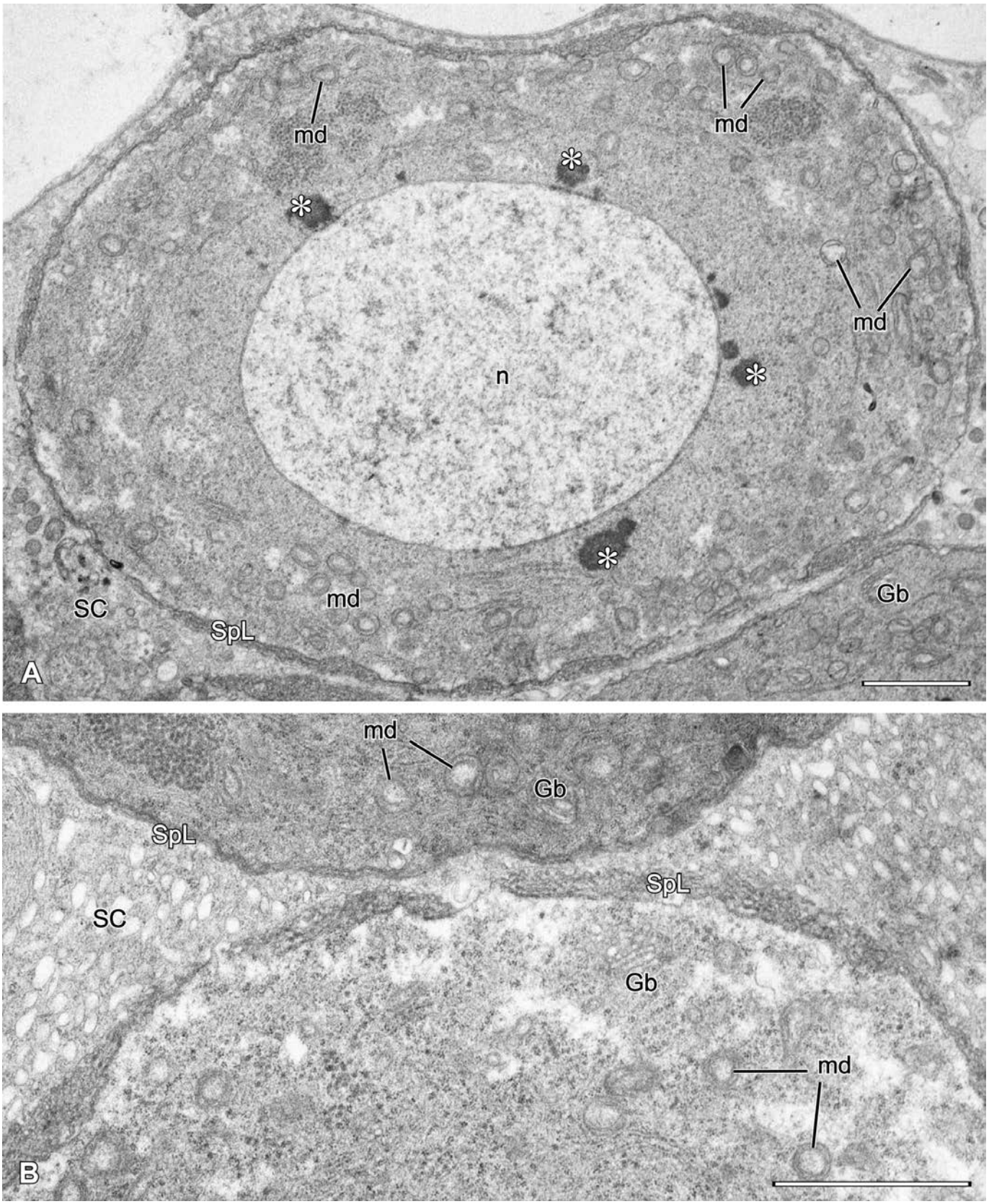


Figure 10 *Chaetodactylus osmiae* male. TEM. (A) Spermatocyte more advanced than those in Figure 9B, embedded in stroma cell (SC). Note thicker spongy layer (SpL) covering the cell surface, large nucleus (n) and nuage material (asterisks). Peripheral cytoplasm contains many mitochondrial derivatives (md): they are roundish and possess one circular crista. A Golgi body (Gb) is present under the spongy layer of a neighboring spermatocyte (right bottom). (B) Peripheral parts of two spermatocytes separated by a stroma cell (SC). Compare the thickness of the spongy layer (SpL) in the upper, less advanced spermatocyte and that of the lower, more advanced cell. Both cells have similar Golgi bodies (Gb) and mitochondrial derivatives (md) but the more advanced, lower spermatocyte shows empty spaces in its peripheral cytoplasm. Scale bars: 2 μm.

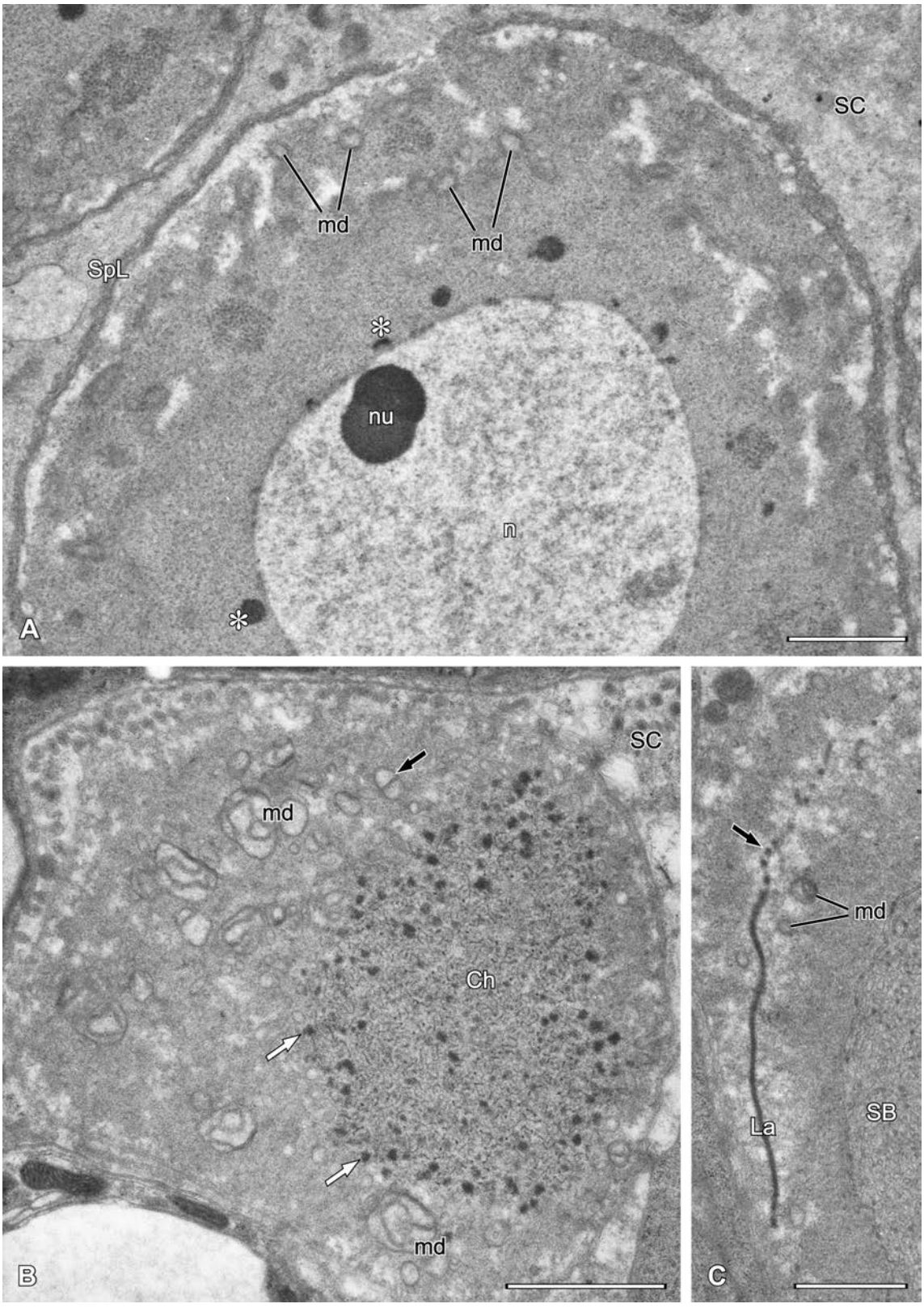


Figure 11 *Chaetodactylus osmiae* male. TEM. (A) Advanced spermatocyte separated with stroma cell (SC) from neighboring spermatocytes. It shows a spongy layer (SpL) and empty spaces in peripheral cytoplasm in which many mitochondrial derivatives (md) are present. Nuage material (asterisks) surrounds the nucleus (n) containing a small, compact nucleolus (nu). (B) Spermatid in an early stage of spermiogenesis embedded in stroma cell (SC). The nucleus is no longer visible and chromatin (Ch) forms fine threads surrounded by foci of electron-dense material (white arrows). Mitochondrial derivatives are multiform, either large with meandering cristae (md) or small and vesicular (black arrow). (C) Section through spermatid at a site where an electron-dense lamella (La) is formed (the arrow indicates a discontinuity in the lamella suggesting the addition of dense material to its margin). Spongy body (SB) derived from the superficial spongy layer of the spermatocyte is also visible. More or less dense mitochondrial derivatives (md) can flank the lamella. Spongy body (SB) derived from the superficial spongy layer of the spermatocyte is also visible. Scale bars: A,B – 2 µm, C – 1 µm.

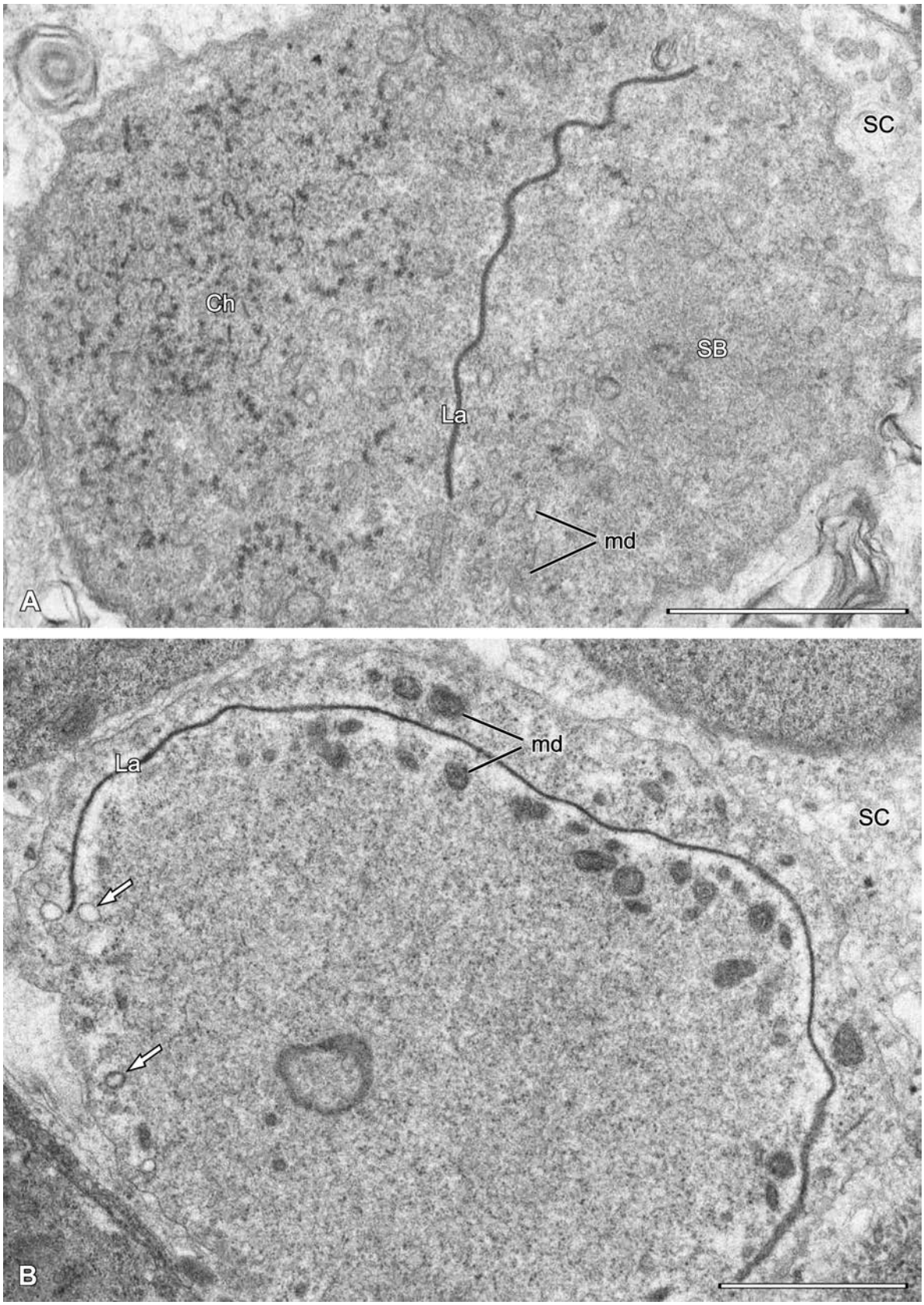


Figure 12 *Chaetodactylus osmiae* male. TEM. Two consecutive steps in spermiogenesis showing spermatid just after lamella (La) formation (A) and subsequently (B) when multiform dense mitochondrial derivatives (md) appear along the lamella. In (A) the spermatid is sectioned through the lamella (La), separating chromatin threads (Ch) and organizing the spongy body (SB). In (B) the spermatid section shows the lamella (La) flanked by dense and multiform mitochondrial derivatives (md). Several small vesicular mitochondrial derivatives can be seen (arrows) close to the left end of the lamella. Scale bars: 2 μm.
Other abbreviations: SC – stroma cell.

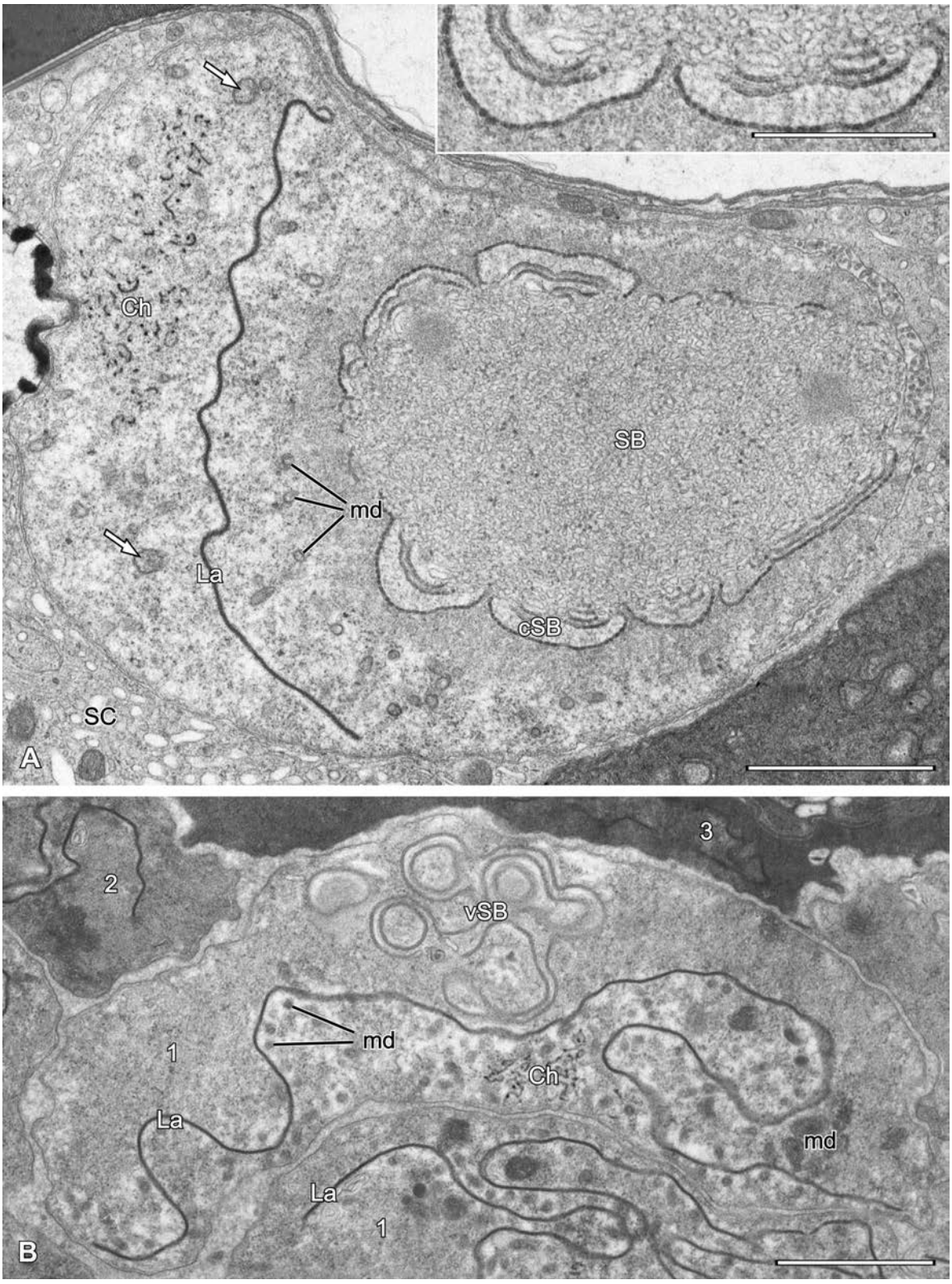


Figure 13 *Chaetodactylus osmiae* male. TEM. (A) Late spermatid showing chromatin threads (Ch), dense lamella (La) and elaborate spongy body (SB). Small vesicles of mitochondrial derivatives (md) are present around the spongy body and along the dense lamella; however, larger and more electron-dense mitochondrial derivatives are also present (arrows). Anastomosing tubules of the spongy body are encircled by characteristic arcuate cisterns (cSB) formed by double membranes similar to annulate lamellae. (Inset) Arcuate cisterns and tubules of spongy body under higher magnification. (B) Two very late spermatids not yet condensed (1) and fragments of finally condensed spermatids (2,3). Each spermatid contains one meandering dense lamella (La) which separates chromatin threads (Ch) from double membrane vesicles (vSB) putatively derived from arcuate cisterns (cSB in A) surrounding the spongy body. Multiform mitochondrial derivatives (md) are frequently located along dense lamella. Scale bars: A,B – 2 µm, A inset – 1 µm.
Other abbreviations: SC – stroma cell.

Spermatogonia that separate from the germarium start to grow and become spherical, with a large spherical nucleus containing a prominent nucleolus either in its center or, more frequently, close to the nuclear envelope (Figs 8B, 9A). The envelope possesses many pores and nuage material in its vicinity. The cytoplasm contains a number of ribosomes, ER profiles, crista-type mitochondria and few Golgi bodies.

During spermatogenesis, mitochondria, ER profiles and Golgi bodies dislocate to the peripheral cytoplasm. Active Golgi bodies provide vesicles which fuse together forming a spongy layer of variable thickness with the plasmalemma (Fig. 9B). Since no signs of meiotic division were observed, we arbitrarily named germ cells surrounded by a spongy layer as spermatocytes (see Discussion). At this time, mitochondria transform gradually into mitochondrial derivatives, at first becoming spherical and with one circular crista. The nucleus and nucleolus are still present, but meandering empty spaces (i.e. unoccupied by ribosomes) appear in the peripheral cytoplasm (Figs 10A-B, 11A).

At the beginning of spermiogenesis the nuclear envelope disappears and nuclear material is visible as thin threads surrounded by electron-dense granules (Fig. 11B). The superficial spongy layer flows to one pole of the cell and then internalises to form a spongy body that is visible as a group of meandering tubular profiles (Figs 11C, 12A, 13A) surrounded by peculiar arcuate cisterns formed by annulated double membranes (Fig. 13A, inset). Some mitochondrial derivatives with distinct cristae are still present, but many diminish to form simplified vesicular structures. The spermatid cytoplasm contains an electron-dense lamella (Fig. 11C) located between two compartments, the chromatin threads and the spongy body (Figs 12A, 13A). In some spermatids, both sides of the lamella are flanked by electron-dense bodies or granules that may be mitochondrial derivatives (Figs 12B, 13B).

Sperm cells found in the male are multiform, approximately 4 x 11 µm, and can represent different stages of condensation (Fig. 13B), increasing with maturity. They contain meandering dense lamella separating the chromatin threads from arcuate cistern profiles, being remnants of spermatid spongy body. Chromatin threads are 45-50 nm thick, whereas the thickness of dense lamella is ca. 45 nm.

Spermatozoa deposited into spermatheca (Fig. 14AB) tightly adhere to each other and show considerable, uniform electron density. The dense lamella is deeply folded and flanked by less condensed cytoplasm containing mitochondrial derivatives of variable shape and density. Chromatin threads are frequently located deeply within the lamella infolding in a subcentral position in the cell (Fig. 14B), but sometimes more marginally (Fig. 14A). A schematic representation of a mature sperm cell (from the spermatheca) is given in Fig. 14C.

Besides spermatozoa, the spermatheca contains large, oval structures of moderate densities of unknown origin (Fig. 1DE).

9. The stroma cells

The number of somatic stroma cells in the male gonad is low as their nuclei are only occasionally observed. The cytoplasm of the stroma cell is less dense than that of germ cells and similar to the ovarian stroma cell, thus containing many vesicular or tubular profiles. Stroma cells fill very narrow spaces between male germ cells with the exception of the germarium and groups of spermatozoa.

Discussion

A recent review on reproductive systems and gametogenesis in astigmatic mites (Witaliński 2014) showed that the female reproductive systems are much less variable than those of males. Accordingly, the female reproductive system in *Ch. osmiae* is very similar to those in other species studied, i.e. it possesses two parts, a primary (the oogenetic) and secondary (the inseminatory) part. Both sections meet at sites where sperm-conveying cords – emerging from the basal part of the spermatheca – reach the ovary surface. The length of sperm-conveying

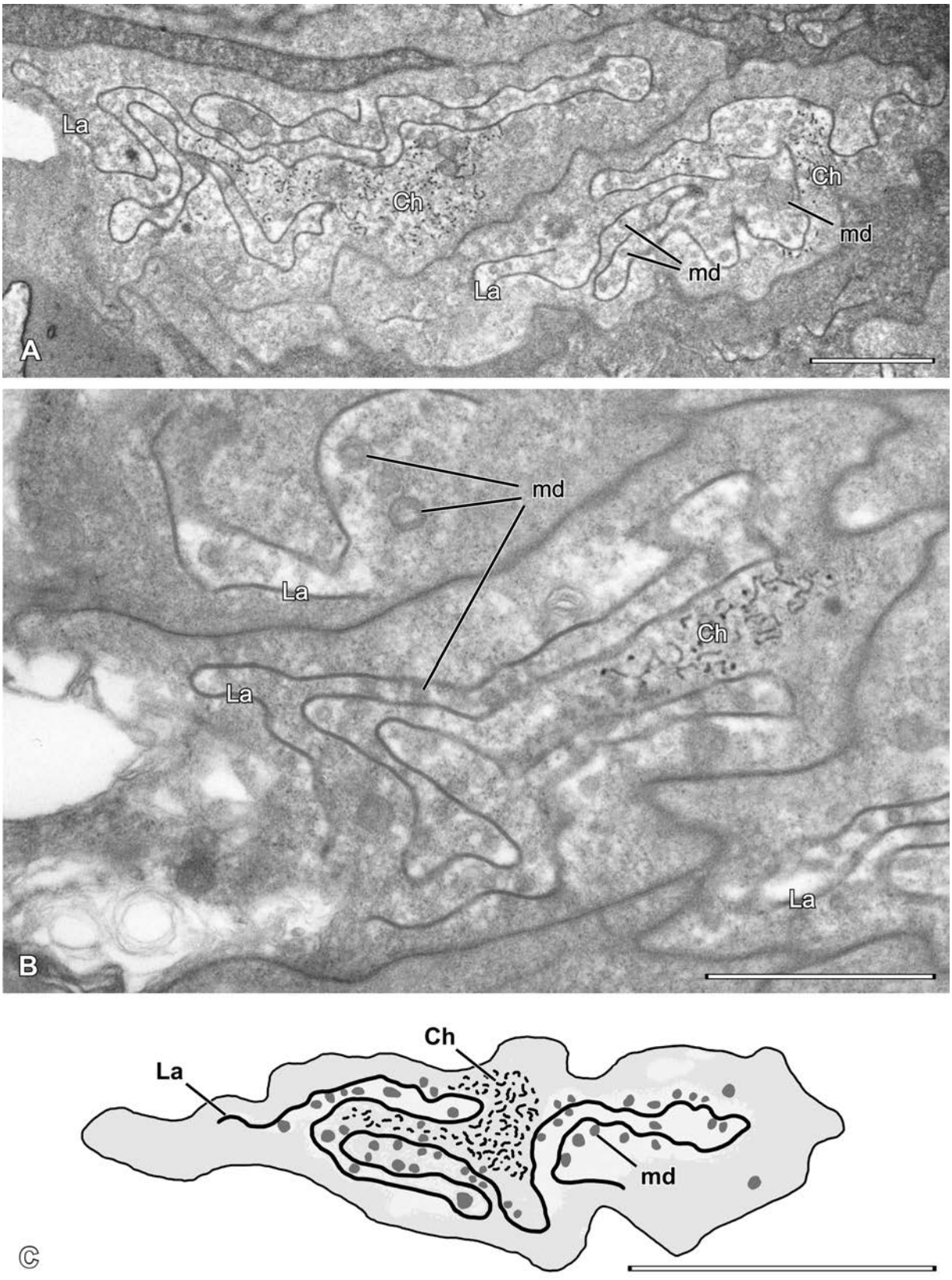


Figure 14 *Chaetodactylus osmiae* female. TEM. Spermatozoa deposited in spermatheca. (A) Two spermatozoa, each with highly folded lamella (La), chromatin (Ch) and mitochondrial derivatives (md). (B) Spermatozoa similar to (A) in higher magnification. Note location of chromatin (Ch) within deep infolding of dense lamella (La). Variable structure of mitochondrial derivatives (md) is also evident. (C) schematic representation of sperm cell from female spermatheca. Scale bars: A,B – 2 μm, C – 5 μm.
Other abbreviations: Ch – threads of chromatin; La – electron-dense lamella; md – mitochondrial derivatives.

cords varies in Astigmata, but is roughly correlated with the length of the inseminatory canal. This is because the position of the spermatheca also varies relative to the posterior end of the idiosoma where the ovaries, the target for sperm cells, are usually located. An extreme example is *Falculifer rostratus,* whose inseminatory canal is up to 300 µm long (Witaliński 2014) and sperm-conveying cords are accordingly very elongated. In *Ch. osmiae* the inseminatory canal is very short and wide, and the basal part of the spermatheca is located just over the ovaries, resulting in minute sperm-conveying cords.

Since Prasse (1968), who first observed the ovarian nutritive cell in Astigmata, this cell was found in all species. However, its location varies within the ovary. The ovaries in the studied species have a large ovarian nutritive cell located in the upper part of the gonad and previtellogenic oocytes are sequestered to its ventral part. This is similar to psoroptidian ovaries, e.g. in *Sarcoptes scabiei* the nutritive cell in the ovary is located either antero-dorsally (Desch 2001) or dorsally in *Notoedres cati* (Witaliński 2014). In *Glycyphagus domesticus*, the location of the nutritive ovarian cell is similar but more variable, either dorsal or subcentral (Witaliński 2014). The function of the nutritive ovarian cell is manifested by an enlarged multilobular nucleus containing many prominent nucleoli, and a cytoplasm rich in ribosomes and other organelles. All early previtellogenic oocytes are connected to the nutritive cell via funnel-type intercellular bridges allowing the delivery of substances from the nutritive cell to oocytes. This type of intercellular bridge is characteristic for Astigmata except for Histiostomatoidea (*Histiostoma, Bonomoia*) where a different type, the diaphragm-crossed bridge, was found (Florek and Witaliński 2010b, Witaliński et al. 2014). Interestingly, *Ch. osmiae* has a very high oviposition rate, producing from 135 up to 515 eggs (from 1.2 to 10.3 eggs daily) during the oviposition period (21 to 46 days) (Chmielewski 1993). However, our study did not show any noteworthy specializations in bridge structure that could be related to a high rate of nutritive cell-oocyte supplementation.

Ovaries in *Ch. osmiae* exhibit two distinctive features: the nutritive ovarian cell possesses numerous protrusions penetrating the surrounding stroma cells, and stroma cells show conspicuous ER cisterns running parallel to contacts of stroma cell and germ-line cells (nutritive cell and oocytes). Protrusions formed by the nutritive cell were also found in *Sarcoptes scabiei* (Desch, 2001) and *Glycyphagus domesticus* (Witaliński 2014), but ER cisterns under the stroma cell surface are unique for the studied species and their role is unknown. We can only speculate that germinal-somatic cell contacts are important and – at least in this species – require enlargement and are possibly equipped with some specializations.

Giant nutritive cells are connected with a large pool of oocytes. We did not observe synaptonemal complexes in nuclei of the earliest germinal cells, suggesting that oogonia entering the meiotic prophase occur in the earlier instar, and in adult females nutritive cell-connected germinal cells are previtellogenic oocytes. This matches observations on gonad development in *Histiostoma* in which meiotic divisions were completed in the tritonymph, thus before the final molt to adult female (Witaliński *et al.* 2014). However, in some species such as *Sancassania berlesei,* the meiotic division is completed much later, in vitellogenic oocytes passing through the middle part of the oviduct (Walzl *et al.* 2004).

A detailed account of vitellogenesis was not an aim of this study, therefore we only provide an initial assessment of this process in *Ch. osmiae.* Vitellogenesis entails autosynthesis and occurs in oviductal oocytes on the basis of materials delivered from the nutritive cell via intercellular bridges and stored in ooplasm, a sequence of events generally accepted for all Astigmata. Typically, vitellogenesis leads to the formation of two types of yolk material, lipid yolk and protein yolk, tightly filling the oocyte. The former consists of lipid droplets associated with glycogen granules, whereas protein yolk forms large spheres with heterogeneous content; some contain electron-lucent paracrystalline inclusions.

During vitellogenesis the oocyte is covered with a vitelline envelope which in this and other species such as *Sancassania anomala* (=*Caloglyphus anomalus*) (Reger 1977) and *Acarus siro* (Witaliński 1993) is lamellar, but later converts into a thinner and homogeneous layer, the chorion (for further discussion on vitelline envelope and chorion origin, as well as chorional

glands in Astigmata, see: Witaliński 2014). It is believed that the entrance of sperm into the oocyte occurs before the development of the vitelline envelope in all Astigmata (Prasse 1968, Witaliński *et al.* 1986, Witaliński 1988) and is correlated with the lack of an acrosomal complex in astigmatan spermatozoa (Liana and Witaliński 2005, Florek and Witaliński 2010a, Witaliński 2014).

The Astigmata reproductive systems in males are more variable than in females (Witaliński 2014). Differences mainly concern the number of testes (unpaired or paired) and their distribution, presence or absence of a testicular central cell in the testis germarium, as well as the number and structure of male accessory glands. In the studied species, the testes are located one-sidedly due to the occupation of the other side of the idiosoma by a large accessory gland as in *Caloglyphus berlesei* (Witaliński and Walzl 1995). In other Astigmata, however, a separate accessory gland is either absent and does not influence the symmetric distribution of the testes, or two glands of different structure are present as in *Lardoglyphus konoi*, leading to the position of one testis in front of the other (Vijayambika and John 1975).

The earliest stages of spermatogenesis are spermatogonia assembled in the germarium. Within the germarium, a conspicuous, so-called testicular central cell may be present. The central cell belongs to the germinal line and in developing gonads is connected to the earliest spermatogonia via tubular intercellular bridges, which later disappear (Witaliński *et al.* 2014). Thus, the testicular central cell seems to be functional in developing testis, but later, it can either remain within the germarium or may deteriorate. The central cell was not observed in the testis of the studied species as in many other Astigmata (Walzl 1992; Witaliński and Walzl 1995; Florek and Witaliński 2010a), although it is present in some species (Prasse 1968; Baker and Krantz 1985; Witaliński *et al.* 1990; Florek and Witaliński 2010a; Witaliński *et al.* 2014). A role for the germarium and testicular central cell in suppressing spermatogonia development has been postulated (for further details see: Witaliński 2014).

Spermatogenesis in Astigmata can proceed in one of two ways, with or without meiotic division, in effect determining the ploidy of males. In haplo-diploid species in which females are diploid and males haploid, arrenotoky occurs and meiosis is absent. Meiosis occurs, however, in diplo-diploid species and two of its consequences can be observed: synaptonemal complexes within prophase nuclei of spermatogonia entering the primary spermatocyte stage, as well as two- or four-cell clonal groups resulting from meiotic divisions. In *Ch. osmiae* neither synaptonemal complexes nor clonal groups of germinal cells were found. This confirms the suggestion by Stanisavljević (1996) that the species is haplo-diploid (with haploid males), which is in contrast to Chmielewski's opinion (Chmielewski 1993) that the species is diplo-diploid.

The absence of meiosis entails a difficulty in defining the spermatocyte stage. For *Ch. osmiae* we used a different criterion to define the spermatocyte stage, as observed in diploid males of Astigmata and Gamasida, in which Golgi bodies contribute to the formation of a distinctive superficial spongy layer enveloping the spermatocyte.

At the beginning of spermiogenesis, meandering membranes of the spongy layer flow to one pole of the cell where they are internalised, forming the so-called spongy body. This conspicuous structure has been found in *Carpoglyphus lactis* (Florek and Witaliński 2010a) and was also reported in *Diplaegidia columbae* (Buchholz) and *Glycyphagus domesticus* (DeGeer) (Witaliński 2014). In some cases (e.g. *Ch. osmiae, G. domesticus*), the spongy body can develop into a quite complex structure of unknown function. In sperm cells, however, only simplified remnants of spongy body can be discerned.

As spermatogenesis proceeds, germ cell mitochondria substantially modify their structure to form roundish bodies containing one circular crista in spermatocytes. Subsequently, however, some undergo structural degradation leading to the formation of smaller electron-dense bodies in which membranes are no longer visible. Despite the occurrence of these mitochondrial derivatives, mitochondria-derived bodies of more conventional structure (i.e. with visible membranes) can still be present even in sperm deposited in the female.

Distinctive characters of Astigmata sperm cells include chromatin threads and electron-dense lamellae. Dense lamellae can be singular, as in *Histiostoma feroniarum* (Liana and

Witaliński 2005), *Carpoglyphus lactis* (Florek and Witaliński 2010a) and *Ch. osmiae*, but are usually multiple and variable in length and distribution (Liana and Witaliński 2005, Witaliński 2014). Their origin is related to the transformation of ER cisterns. In the case of *Ch. osmiae,* the origin of singular dense lamella was not observed in detail, but some images (Fig. 11C) suggest the formation of focal densities within lamella margins. Such densities can later coalesce to form the dense filling of lamella. The role of dense lamellae is still under speculation, but since sperm chromatin is frequently surrounded by the lamella(e), the mechanic protection of genetic material may be an explanation. In *Ch. osmiae,* the dense lamella of inseminating spermatozoa is folded many times over, and chromatin threads frequently occupy a central position in such infoldings. Some protection of chromatin material seems to be beneficial since in most Astigmata the sperm is delivered into the female spermatheca under considerable pressure, first through a narrow male ejaculatory duct and then through the female inseminatory duct. Furthermore, spermatozoa crawl via sperm-conveying cords from the spermatheca to ovaries which can lead to a high incidence of deformation. Therefore some unusual characters of Astigmata sperm including 1) multiform shape of spermatozoa, 2) chromatin in threads instead of in a rigid nucleus, and 3) the central location of the chromatin sheltered by electron-dense lamellae, can be explained as an adaptive response to mechanical stress during and after insemination (Witaliński 2014). In the *Ch. osmiae* female, the inseminatory duct is short and wide and sperm-conveying cords are minute. Therefore, the main source of mechanical stress to spermatozoa may be the pumping of sperm by the male through the narrow (diameter ca. 2 μm) ejaculatory duct.

Conclusions

Female and male reproductive systems in *Chaetodactylus osmiae* match the general features of other astigmatan species. The female reproductive system and ovary structure is typical and differs only in details from other species studied to date. The functional structure of intercellular bridges coupling the ovarian nutritive cell and previtellogenic oocytes, and also the chemical details of vitelline envelope transformation into the chorion remain to be established. Furthermore, additional characteristics of the chorion are needed to develop potential methods of mite control.

In the male, the course of spermatogenesis confirms arrhenotoky in this species, whereas sperm structure is similar to that of other Astigmata. In the future, detailed studies on the formation of the heterogeneous, male-derived material deposited in the spermatheca, containing spermatozoa but also large globular structures, are planned to better describe the functioning of the spermatheca.

Acknowledgments

The authors wish to thank Prof. Dr. Michał Woyciechowski (Institute of Environmental Sciences, Jagiellonian University) for supplying *Chaetodactylus osmiae* for studies, as well as to Dr. Dagmara Podkowa for perfect technical assistance in TEM. TEM observations were done in the Department of Cell Biology and Imaging, Institute of Zoology and Biomedical Research, Jagiellonian University. The English of the MS was kindly corrected by Dr. Maciej Pabijan, Institute of Zoology and Biomedical Research, Jagiellonian University. The work was supported by DS Grant K/ZDS/006307 and K/ZDS/007345 (funds for statutory activities of the Jagiellonian University).

References

Baker G.T., Krantz G.W. 1985. Structure of the male and female reproductive and digestive systems of *Rhizoglyphus robini* Claparède (Acari, Acaridae). Acarologia 26: 55-65.

Bosch J. 1992. Parasitism in wild and managed populations of the almond pollinator *Osmia cornuta* (Latr.) (Hymenoptera, Megachilidae). J. Apicult. Res. 31: 77-82. doi:10.1080/00218839.1992.11101266
Chmielewski W. 1993. Biology of *Chaetodactylus osmiae* (Duf., 1866) (Acarida, Chaetodactylidae) – polleneater phoretic on solitary bees (Apoidea). Pszczelnicze Zeszyty Naukowe, 37: 133-143. [in Polish, with English Summary]
Desch C.E. 2001. Anatomy and ultrastructure of the female reproductive system of *Sarcoptes scabiei* (Acari: Sarcoptidae). In: Acarology: Proceedings of the 10th International Congress (R.B. Halliday, D.E. Walter, H.C. Proctor, R.A. Norton and M.J. Colloff Eds.), CSIRO Publications, Collingwood, pp. 203-212.
Fain A. 1966. Notes sur la biologie des acariens du genre *Chaetodactylus* et en particulier de *C. osmiae*, parasite des abeilles solitaires *Osmia rufa* et *O. cornuta* en Belgique (Sarcoptiformes: Chaetodactylidae). Bull. Anals. Soc. r. belge. Ent. 102: 251-261.
Florek M., Witaliński W. 2010a. Spermatogenesis and sperm structure in *Carpoglyphus lactis* (L.) (Acari: Astigmata). Arthropod Struct. Dev. 39: 41-51. doi:10.1016/j.asd.2009.09.001
Florek M., Witaliński W. 2010b. Intercellular bridges in ovaries of astigmatic mites: their fine and molecular structure (Acari: Astigmata). In: XIII International Congress of Acarology – Abstract Book (G.J. de Moraes, R.C. Castilho and C.H.W. Flechtmann Eds.), Recife, Brazil, August 23-27, 2010, p. 87.
Karnovsky M.J. 1965. A formaldehyde–glutaraldehyde fixative of high osmolarity for use in electron microscopy. J. Cell Biol. 27: 137A-138A.
Klimov P.B., OConnor B., Ochoa R., Bauchan G.R., Redford A.J., Scher J. 2016. Bee Mite ID: Bee-Associated Mite Genera of the World. USDA APHIS Identification Technology Program (ITP), Fort Collins, CO. Available from http://idtools.org/id/mites/beemites.Accessed5/09/2017.
Krunić M., Pinzauti M., Felicioli A., Stanisavljevic L.J. 1995. Further observations on *Osmia cornuta* Latr. and *O. rufa* L. as alternative fruit pollinators, domestication and utilization. Arch. Biol. Sci. 47: 59-66.
Krunić M., Stanisavljević L., Brajković M., Tomanović Ž., Radović I. 2001. Ecological studies of *Osmia cornuta* (Latr.) (Hymenoptera, Megachilidae) populations in Yugoslavia with special attention to their diapause. Acta Hortic. 561: 297-301. doi:10.17660/ActaHortic.2001.561.45
Krunić M., Stanisavljević L., Pinzauti M., Felicioli A. 2005. The accompanying fauna of *Osmia cornuta* and *Osmia rufa* and effective measures of protection. Bull. Insectology 58: 141-152.
Liana M., Witaliński W. 2005. Sperm structure and phylogeny of Astigmata. J. Morphol. 265: 318-324. doi:10.1002/jmor.10361
Michael A.D. 1903. British Tyroglyphidae. Roy. Society, London, Vol. 2, pp. 12-28.
Norton R.A. 1998. Morphological evidence for the evolutionary origin of Astigmata (Acari: Acariformes). Exp. Appl. Acarol. 22: 559-594. doi:10.1023/A:1006135509248
OConnor B.M. 1984. Phylogenetic relationships among higher taxa in the Acariformes, with particular reference to the Astigmata. In: Acarology VI (D.A. Griffiths and C.E. Bowman Eds.), Ellis-Horwood, Chichester, UK, pp. 19-27.
OConnor B.M. 2009. Cohort Astigmatina. In: A Manual of Acarology (G.W. Krantz and D.E. Walter Eds.), Texas Tech University Press, Lubbock, pp. 565-657.
OConnor B.M., Klimov P. 2009. North American Bee-Associated Mites. USDA, the Cooperative State Research, Education and Extension Service. Available from http://insects.ummz.lsa.umich.edu/beemites/Species_Accounts/Chaetodactylus.htm. Accessed 20/10/2017.
Prasse J. 1968. Untersuchungen über Oogenese, Befruchtung, Eifurchung und Spermatogenese bei *Caloglyphus berlesei* (Michael, 1903) und *Caloglyphus michaeli* (Oudemans, 1924) (Acari: Acaridae). Biol. Zbl. 87: 757-775.
Reger J.F. 1977. A fine structure study on vitelline envelope formation in the mite, *Caloglyphus anomalus*. J. Submicrosc. Cytol. 9: 115-125.
Schatz H., Behan-Pelletier V.M., OConnor B.M., Norton R.A. 2011. Suborder Oribatida van der Hammen, 1968. In: Animal Biodiversity: An Outline of Higher-level Classification and Survey of Taxonomic Richness (Z.-Q. Zhang, Ed.). Zootaxa 3148: 141-148.
Stanisavljević L. 1996. The impact of accompanying fauna on the populations of newly domesticated solitary bees *Osmia cornuta* (Latr.) and *O. rufa* (L.) (Megachilidae,
Van Asselt L. 2000. Observations on the life cycle of *Chaetodactylus osmiae* (Dufour, 1839) (Acari: Chaetodactylidae) parasitic on the solitary bee, *Osmia rufa* (L.), 1758 (Insecta: Hymenoptera) in Belgium. Internat. J. Acarol. 26: 221-228. doi:10.1080/01647950008684192
Velthuis H.H.W., Van Doorn A. 2006. A century of advances in bumblebee domestication and the economic and environmental aspects of its commercialization for pollination. Apidologie 37: 421-451.
Venable J.H., Coggeshall R. 1965. A simplified lead citrate stain for use in electron microscopy. J. Cell Biol. 25: 407-408. doi:10.1083/jcb.25.2.407
Vijayambika V., John P.A. 1975. Internal morphology and histology of the fish mite *Lardoglyphus konoi* (Sasa and Asanuma) (Acarina: Acaridae). 2. The reproductive system. Acarologia 17: 106-113.
Walzl M.G. 1992. Ultrastructure of the reproductive system of the house dust mites *Dermatophagoides farinae* and *D. pteronyssinus* (Acari, Pyroglyphidae) with remarks on spermatogenesis and oogenesis. Exp. Appl. Acarol. 16: 85-116. doi:10.1007/BF01201494
Walzl M.G., Gutweniger A., Wernsdorf P. 2004. Embryology of mites: new techniques yield new findings. Phytophaga 14: 163-181.
Witaliński W. 1988. Spermatogenesis and postinseminational alterations of sperm structure in a sarcoptid mite, *Notoedres cati* (Hering) (Acari, Acaridida, Sarcoptidae). Acarologia 29: 411-421.
Witaliński W. 1993. Egg shells in mites: vitelline envelope and chorion in Acaridida (Acari). Exp. Appl. Acarol. 17: 321-344. doi:10.1007/BF00058596

Witaliński W. 2014. Gonads and gametogenesis in astigmatic mites (Acariformes: Astigmata). Arthropod Struct. Dev. 43: 323-340. doi:10.1016/j.asd.2014.04.003
Witaliński W., Walzl M.G. 1995. Reproductive systems in selected acaridid mites (Acaridida). In: The Acari. Physiological and Ecological Aspects of Acari-Host Relationships (D. Kropczyńska, J. Boczek and A. Tomczyk Eds.), Dabor, Warszawa, pp. 109-116.
Witaliński W., Jończy J., Godula J. 1986. Spermatogenesis and sperm structure before and after insemination in two acarid mites, *Acarus siro* L. and *Tyrophagus putrescentiae* (Schrank) (Acari: Astigmata). Acarologia 27: 41-51.
Witaliński W., Szlendak E., Boczek J. 1990. Anatomy and ultrastructure of the reproductive systems of *Acarus siro* (Acari: Acaridae). Exp. Appl. Acarol. 10: 1-31. doi:10.1007/BF01193970
Witaliński W., Rożej-Pabijan E., Podkowa D. 2014. Gonads in *Histiostoma* mites (Acariformes: Astigmata): Structure and development. Arthropod Struct. Dev. 43: 385-401. doi:10.1016/j.asd.2014.04.006